ELSEVIER

www.elsevier.nl/locate/jorganchem

Journal of Organometallic Chemistry 595 (2000) 166–177

Journal of Organometallic Chemistry

Preparation, properties and reactions of metal-containing heterocycles
Part C: tetraazatetraphosphadimolybdacyclophanes: synthesis, isolation, characterization, and X-ray crystal structures☆

Ekkehard Lindner [a,*], Markus Mohr [a], Christiane Nachtigal [a], Riad Fawzi [a], Gerald Henkel [b]

[a] *Institut für Anorganische Chemie der Universität Tübingen, Auf der Morgenstelle 18, D-72076 Tübingen, Germany*
[b] *Institut für Synthesechemie der Universität (GH) Duisburg, Lotharstraße 1, D-47057 Duisburg, Germany*

Received 14 July 1999; received in revised form 20 August 1999; accepted 9 September 1999

Dedicated to Professor Alfred Schmidpeter on the occasion of his 70th birthday.

Abstract

The ditopic aminodiphosphines $CH_2(4,4'\text{-}Ph_2PNHC_6H_4)_2$ (**2**) and $CH_2(4,4'\text{-}Ph_2PCH_2NHC_6H_4)_2$ (**5**) are obtained by reaction of 4,4′-diaminodiphenylmethane with $ClPPh_2$ and (i) $(CH_2O)_n$/NaOMe/(ii) $HPPh_2$, respectively. Treatment of $(\eta^4\text{-nbd})Mo(CO)_4$ with **2** and **5** under high-dilution conditions in CH_2Cl_2 affords the tetraazatetraphosphadimolybdaclophanes $[CH_2(4,4'\text{-}(OC)_4Mo(Ph_2PNHC_6H_4)_2)]_2$ (**3**) and $[CH_2(4,4'\text{-}(OC)_4Mo(Ph_2PCH_2NHC_6H_4)_2)]_2$ (**6**) in relatively high yields. The structures of **3** and **6** were investigated by X-ray crystal-structure analyses. Whereas the cavity of the molecular structure of **3** can be described by a parallelogram, that of **6** has the shape of a boat in which the diphenylmethane building blocks form the hull and the *cis*-$(Ph_2P)_2Mo(CO)_4$ fragments represent the bow and stem, respectively. Because of the formation of only very weak hydrogen bonds in **3** and **6**, no binding to molecules like *p*-benzoquinone, 1,4-cyclohexanedione, 2,5-piperazinedione and *trans*-1,4-diaminocyclohexane could be detected. © 2000 Elsevier Science S.A. All rights reserved.

Keywords: Dimolybdacyclophanes; Molybdenum complexes; Aminophosphines; Macrocyclization; High dilution

1. Introduction

Cyclophanes play an important role in the development of supramolecular chemistry [2]. However, research has been mainly focused on cyclophanes with a mere organic ring skeleton. Typical examples are provided by calixarenes [3] cryptophanes [4], carcerands and hemicarcerands [5]. In recent years transition metal centers have become the focal point of interest. The incorporation of metal fragments not only enables the phenomenon of self-assembly to occur [6], but also affords cyclophanes with properties like catalytic [7] or redox activity [8], Lewis acidity [9], luminescence [10] and paramagnetism [11]. These features may exert a remarkable impact on the chemical and physical behavior of such cyclophanes [12]. Furthermore the insertion of complex moieties influences the structure of metallacyclophanes because of their steric requirements and they can serve as reactive centers for the binding of molecules or as sensors for an included guest [13]. The bis(triflate) method — a variant of cationic alkylation — is an excellent method for the concomitant formation of several metal–carbon σ bonds. It proved to be suitable for the synthesis of several ferra- and osmacyclophanes [14]. However, this method cannot be successfully applied if heteroatoms (S, N, O) are present in the hydrocarbon framework [15].

An alternative approach to metallacyclophanes refers to the well-developed phosphine chemistry. The objec-

* Corresponding author. Tel.: +49-707-129-72039; fax: +49-707-129-5306.
E-mail address: ekkehard.lindner@uni-tuebingen.de (E. Lindner)
☆ Part IC: see Ref. [1].

PII: S0022-328X(99)00587-2

tive in this investigation was the synthesis of ditopic phosphine ligands with secondary amino functionalities and diphenylmethane building blocks that are known to preorganize cavities. These novel ligands were reacted with a suitable transition metal precursor in a 2:2 cyclization reaction under high dilution conditions to generate dimolybdacyclophanes with NH-binding sites. Such cyclophanes have the potential to act as host molecules [16].

2. Results and discussion

2.1. Synthesis of ligands 2 and 5

For a largely quantitative reaction the treatment of the diamine **1** with $ClPPh_2$ has to be carried out in the presence of the auxiliary base NEt_3 [17] (Scheme 1). Stronger bases, like *n*-butyllithium, are not successful, because the lithiated diamine **1** deprotonates **2** as soon as it is formed, leading to undesired by-products. Because of its thermal and hydrolytic sensitivity, the arylaminophosphine **2** cannot be purified by common methods (distillation, chromatography) [18], hence it must be washed with a dilute aqueous solution of $NaHCO_3$. The ligand **2** crystallizes with 1 mol of water and its composition was established by an FD mass spectrum, revealing the molecular peak at $m/z = 566$. Compound **2** is a colorless air-stable solid, which is indefinitely storable at -18°C and dissolves readily in organic solvents of medium polarity. In halogenated solvents a slow decomposition takes place.

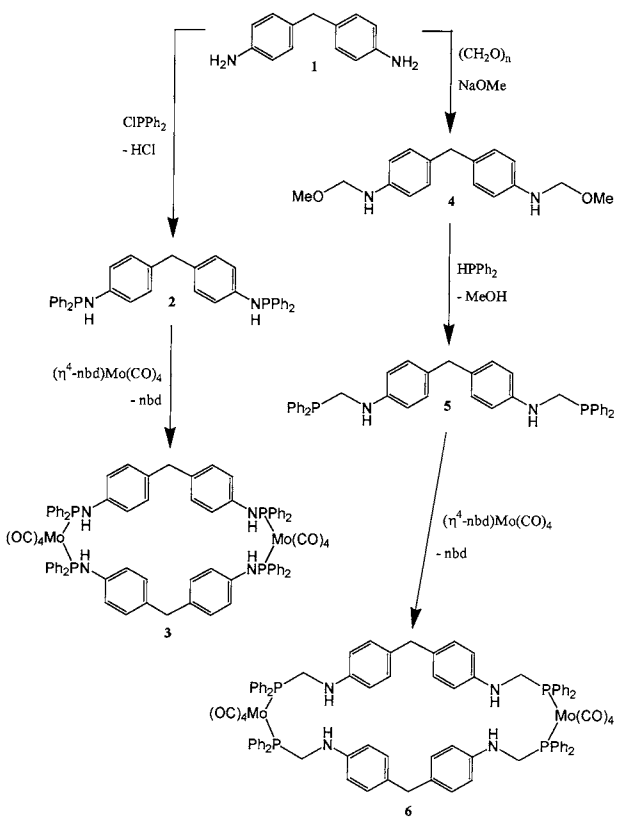

Scheme 1. Synthesis of the aminophosphines **2** and **5** and the dimolybdacyclophanes **3** and **6**.

For access to the arylaminomethylphosphine **5** an intermediate step has to be considered (Scheme 1). First the diamine **1** is converted into the corresponding methoxymethylamine **4** by reaction of paraformaldehyde with NaOMe in methanol. However, in contrast to the monofunctional methoxymethylamines described by Barluenga et al. [19], the bifunctional amine **4** cannot be isolated by removing the solvent, because even at low temperatures a polymerization takes place. Subsequently the in situ product **4** was immediately reacted with excess diphenylphosphine in dichloromethane to give the arylaminomethylphosphine **5**, which after work up precipitates as a colorless, air-stable solid. The diphos ligand **5** readily dissolves in solvents of medium polarity, but ethers induce polymerization. An FD mass spectrum corroborated the expected composition of this ligand, showing the molecular peak at $m/z = 595$.

The $^{31}P\{^1H\}$-NMR spectra of the diphosphines **2** and **5** (in $CDCl_3$) exhibit a singlet at δ 29.5 and -17.9, respectively. In the low- and high-field region both ^1H-NMR spectra ($CDCl_3$) display one AB pattern (**2**: δ 7.0 and 6.9; **5**: δ 7.0 and 6.5) and a singlet (δ 3.7), which are assigned to the aromatic and methylene protons of the diphenylmethane unit. A doublet in the spectrum of **5** at δ 3.8 is attributed to the protons of the methylene group between nitrogen and phosphorus. Whereas the ^1H-NMR spectrum of **2** is characterized by a doublet for the NH function at δ 4.2, the NH group in **5** gives rise to a broad singlet at δ 3.5. The IR spectra of the ligands **2** and **5** (THF) show absorptions at 3289 and 3351 cm^{-1}, respectively, which are ascribed to N–H stretching vibrations.

2.2. Synthesis of the dimolybdacyclophanes 3 and 6

To promote the formation of the dinuclear dimolybdacyclophanes **3** and **6** (Scheme 1) two preconditions have to be fulfilled. (i) The divergent properties of the diphosphine ligands **2** and **5** require a convergent metal fragment that prearranges the coordination geometry precisely. (ii) The thermal lability of the employed ligands **2** and **5** necessitates a coreactant that reacts as fast as possible at ambient temperature. Both prerequisites are best complied with the application of (η^4-nbd)$Mo(CO)_4$.

The reactions between (η^4-nbd)$Mo(CO)_4$ and **2** and **5**, respectively, are carried out under high-dilution conditions in dichloromethane [20]. To meet this requirement a computer-controlled dosing apparatus was constructed, which allows a highly synchronous addi-

tion of the solutions of two sensitive reactants into a reaction flask in any desired rate and under exclusion of light [21]. With the aid of such an apparatus it was possible to double the yields of the expected tetraazatetraphosphadimolybdacyclophanes.

The favored formation of the dinuclear molybdacyclophanes **3** and **6** may be rationalized by the following course of reaction: in a first step a diphosphine ligand attacks nucleophilically (η^4-nbd)$Mo(CO)_4$ to give an open-chain mononuclear intermediate with one phosphine and one (η^2-nbd)$Mo(CO)_4$ end group each [22]. Owing to the steric conditions of the diphosphines **2** and **5**, both phosphorus donors are not able to coordinate to a single transition metal fragment. Thus ring closure is not possible at this stage and the formation of cyclic mononuclear species is unlikely. In a second S_N-type reaction two mononuclear units react with each other to give a dinuclear open-chain intermediate with the same above-mentioned end groups. In principle this dinuclear species can undergo an intramolecular cyclization or it reacts intermolecularly either with a further diphosphine and a (η^4-nbd)$Mo(CO)_4$ molecule, respectively, or with itself to give open-chain products. The formation of non-cyclic compounds or ring systems of higher nuclearity is partially or largely suppressed if the dilution principle is adhered to as strictly as possible by employing the mentioned dosing apparatus. Only in this case do the ends of the dinuclear chains have enough time to approach each other in a cyclic conformation. Once a tri- or tetranuclear chain is formed it will react to give oligo- or polynuclear rings or open-chain by-products.

Unlike the ligands **2** and **5**, the corresponding colorless dimolybdacyclophanes **3** and **6** are rather stable toward oxygen and moisture and dissolve slowly in dichloromethane and chloroform, respectively. The solutions are slightly sensitive to light and the purification of **3** and **6** succeeded via middle-pressure liquid chromatography (MPLC).

Compared to the $^{31}P\{^1H\}$-NMR spectra of **2** and **5**, the $^{31}P\{^1H\}$ signals of the dimolybdacyclophanes (**3** in $CDCl_3$; **6** in CD_2Cl_2) are shifted to lower field [23]. The ^1H-NMR spectra of **3** and **6** are quite similar to those of the ligands **2** and **5**. The observation of a degenerate AA′BB′ system is a consequence of the fast rotation of the phenylene rings within the diphenylmethane units. Even at -55°C this effect could not be frozen out. A doublet of triplets is observed in the spectrum of the dimolybdacyclophane **6** at δ 3.5, which is attributed to the NH protons. A $^1H\{^{31}P\}$-NMR experiment reduces the spectrum to a simple triplet, typical for a coupling of the NH to the vicinal CH_2 protons. In the case of the smaller dimolybdacyclophane **3** only a complex multiplet at δ 4.6 is observed for the NH protons. This multiplet is generated by an AA′XX′ spin system. ^{31}P decoupling results in the expected singlet. Between 2025 and 1880 cm^{-1} the IR spectra of **3** and **6** exhibit four CO absorptions (**3** in CCl_4, **6** in acetone), which is consistent with the presence of *cis*-$Mo(CO)_4$ arrangements. The NH stretching vibration in the IR spectrum of **6** is found in the same region as that of the ligand **5**. In the case of the smaller dimolybdacyclophane **3** two NH absorptions are observed: a sharp peak at 3389 and a broad band at 3245 cm^{-1}, indicating N–H···N hydrogen bonds [24]. Dilution experiments did not change the intensity ratio of these two absorptions, i.e. the hydrogen bonds were not cleaved revealing their intramolecular character.

The separated remainders of the reaction mixtures showed absorptions of *cis*-$Mo(CO)_4$ groups in the IR spectra and low-field shifted signals in the $^{31}P\{^1H\}$-NMR spectra, which are in a similar range as those for **3** and **6**. These observations point to higher nuclear or polynuclear species. According to the MPLC chromatograms, several small fractions were observed. With increasing retention time these fractions become smaller and their separation becomes more complicated.

2.3. X-ray crystal structures of the dimolybdacyclophanes *3* and *6*

To get a more detailed structural information about the dimolybdacyclophanes, X-ray structural analyses were performed. ORTEP drawings of the molecular structures of **3** and **6** with atom labeling are depicted in Fig. 1 (top) and 4 (top). A listing of selected bond lengths and angles is summarized in Tables 1 and 2. The cavity of the molecular structure of **3** can be described by a parallelogram. The vertices of this parallelogram are occupied by the atoms Mo(3), C(12), Mo(3A), and C(12A). The lengths of the edges are 9.278(7) (Mo(3)–C(12)) and 9.162(6) Å (Mo(3)–C(12A)) with angles of 93.47(5)° (P(2)–Mo(3)–P(4)) and 112.0(5)° (C(13)–C(12)–C(9A)). The diagonals of this parallelogram, which represent the Mo(3)–Mo(3A) and C(12)–C(12A) distances, have lengths of 15.106(2) and 10.58(1) Å. Both diphenylmethane units in **3** are oriented face-to-face and generate a cylindrical cavity, because the opposite carbon atoms are connected by a center of inversion. Within a diphenylmethane building block the phenylene rings are not perpendicular to the plane, which is defined by the atoms C(9A), C(12), and C(13). The deviations from the vertical orientation are 7.4(2) and 11.8(2)°.

A space-filling model (Fig. 1, bottom) demonstrates that the interior of the cyclophane framework is big enough to include guest molecules with an adequate dimension. Indeed, one disordered $CHCl_3$ molecule is included inside this cavity, and five disordered $CHCl_3$ molecules are located outside. Each phenyl substituent of the four $P(C_6H_5)_2$ units is partially shielding the entrance of the cavity. Consequently the NH functions

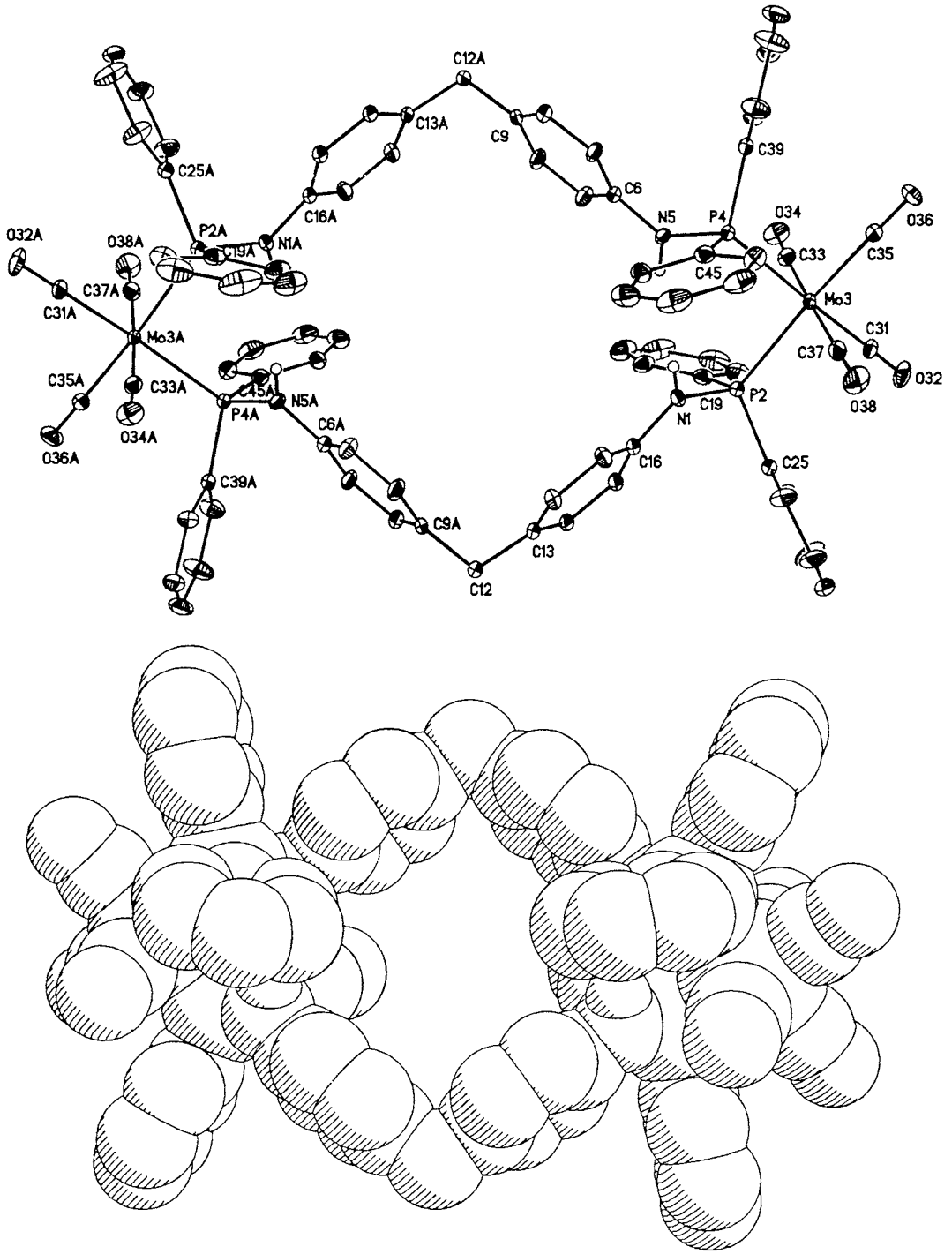

Fig. 1. Top: ORTEP plot of the molecular structure of compound **3**. Thermal ellipsoids are drawn at 20% probability level, except for H atoms. Phenyl rings are numbered cyclically. Bottom: space-filling representation of **3**. Solvent molecules are omitted for clarity.

are completely hidden by these phenyl rings. Furthermore it is remarkable that both NH groups at each side of a diphenylmethane unit are either oriented above or below the cavity, but not inside. To bind guest molecules inside the cavity via hydrogen bonding, a change in the conformation of **3** would be necessary.

The shielding of the cavity by the P-phenyl rings is corroborated by an inspection of the packing mode of the molecules of **3** (Fig. 2). Along the *a* axis these molecules form continuous channels with their cavities and the above-mentioned phenyl rings point to the centers of the channels, thus impeding free passage. The smallest distance between these phenyl rings is 5.177(2) Å (C(21A)–C(49)).

To demonstrate the influence of both *cis*-$(Ph_2P)_2Mo(CO)_4$ fragments on the geometry of the

Table 1
Selected interatomic distances (Å) and interbond angles (°) for **3**

Interatomic distances			
Mo(3)–C(12)	9.278(7)	P(2)–N(1)	1.689(5)
Mo(3)–C(12A)	9.162(6)	P(4)–N(5)	1.689(5)
Mo(3)–Mo(3A)	15.106(2)	N(1)–C(16)	1.414(8)
C(12)–C(12A)	10.58(1)	N(5)–C(6)	1.412(7)
C(21A)–C(49)	5.177(2)	C(9)–C(12A)	1.512(8)
Mo(3)–P(2)	2.500(2)	C(12)–C(13)	1.512(9)
Mo(3)–P(4)	2.510(1)		
Interbond angles			
P(2)–Mo(3)–P(4)	93.47(5)	C(45)–P(4)–Mo(3)	115.3(2)
C(13)–C(12)–C(9A)	112.0(5)	C(39)–P(4)–Mo(3)	115.6(2)
C(33)–Mo(3)–C(37)	177.7(2)	N(1)–P(2)–C(19)	106.3(3)
P(2)–Mo(3)–P(4)	93.47(5)	N(1)–P(2)–C(25)	102.6(3)
N(1)–P(2)–Mo(3)	114.5(2)	C(19)–P(2)–C(25)	105.2(3)
C(16)–N(1)–P(2)	131.7(4)	C(45)–P(4)–C(39)	104.5(3)

cavity, it is appropriate to compare **3** with the likewise 28-membered diosma[5.1.5.1]paracyclophane [14a]. Similar to **3** this macrocycle contains two 4,4′-substituted diphenylmethane units, which are connected to two *cis*-$Os(CO)_4$ fragments via two methylene groups. The absence of the voluminous diphenylphosphino groups in the diosma[5.1.5.1]paracyclophane affects the shape of the cavity: the Os(1)–Os(2) distance (12.334(4) Å) is smaller and the distance between the methylene carbon atoms bridging the phenylene rings (12.224(1) Å) is larger as compared to the corresponding distances in **3** (15.106(2) and 10.58(1) Å). In other words, the cavity in **3** is extended along the Mo(3)–Mo(3A) axis. This can be explained as follows: on the basis of X-ray structural data Fig. 3 displays a schematic view of the transition metal fragments of both the diosma-[5.1.5.1]paracyclophane and **3** along the axial CO ligands. The depicted orientations of the β bonds in **3** result if the α bonds in the diosma[5.1.5.1]-paracyclophane being rotated by 180°. From this it follows that in **3** the β bonds are oriented inwards, which lengthens the Mo(3)–Mo(3A) and narrows the C(12)–C(12A) distances, thus the cavity of **3** is contracted. In contrast to **3** in the diosma[5.1.5.1]paracyclophane the β bonds are oriented outwards, which shortens the Os(1)–Os(2) and lengthens the C(17)–C(34) distance. In this case the cavity nearly adopts the shape of a rectangle. The reason for this rotation is quite obvious. The orientation of the β bonds in the diosma[5.1.5.1]paracyclophane suggests that the substituents at the α-carbon atoms (two hydrogen atoms) are located inside the cavity. This conformation is impossible in the case of **3**, because each α-phosphorus atom is provided with two bulky phenyl groups, which repel each other. These phenyl rings adopt the optimum distance by such a rotation of the α bonds, that one phenyl ring is oriented either above or below and the other one sidewards away from the cavity.

Table 2
Selected interatomic distances (Å) and interbond angles (°) for **6**

Interatomic distances			
Mo(4)–Mo(4A)	15.338(4)	N(1)–C(2)	1.439(7)
C(14)–C(14A)	6.397(3)	N(7)–C(6)	1.432(8)
Mo(4)–P(3)	2.524(1)	N(1)–C(19)	1.396(8)
Mo(4)–P(5)	2.537(2)	N(7)–C(8)	1.405(7)
P(3)–C(2)	1.859(6)	C(11)–C(14)	1.529(7)
P(5)–C(6)	1.854(5)	C(14)–C(15)	1.500(8)
Interbond angles			
P(3)–Mo(4)–P(5)	91.54(4)	C(8)–N(7)–C(6)	121.2(5)
C(2)–P(3)–Mo(4)	111.7(2)	C(15)–C(14)–C(11)	114.3(5)
C(6)–P(5)–Mo(4)	120.3(2)	C(33)–Mo(4)–C(39)	175.3(3)
N(1)–C(2)–P(3)	107.9(3)	C(27)–P(3)–C(21)	96.7(3)
C(41)–P(5)–Mo(4)	113.6(2)	C(47)–P(5)–C(41)	104.7(3)
C(47)–P(5)–Mo(4)	116.6(2)	C(27)–P(3)–Mo(4)	120.1(2)
N(7)–C(6)–P(5)	110.1(4)	C(21)–P(3)–Mo(4)	120.2(2)
C(19)–N(1)–C(2)	120.5(4)		

A comparison of the axial CO ligands is quite interesting. Whereas in the diosma[5.1.5.1] paracyclophane they are inclined toward the cavity (CO_{ax}–CO_{ax} = 165.2(4)°) due to the electropositive alkyl chains [25], they are inclined in the opposite direction in **3** (CO_{ax}–CO_{ax} = 177.7(2)°).

In contrast to **3**, the molecular structure of the 32-membered dimolybdacyclophane **6** represents roughly the shape of a boat in which the diphenylmethane building blocks form the hull and the *cis*-$(Ph_2P)_2Mo(CO)_4$ fragments the bow and stem, respectively (Fig. 4, top). The Mo(4)–Mo(4A) and C(14)–C(14A) distances are 15.338(4) and 6.397(3) Å. Again the phenylene rings are not perpendicular to the plane in which the atoms C(11), C(14) and C(15) are located. The deviations from the vertical position are 25.0(2) and 7.8(2)°. Unlike in **3**, the diagonally opposite phenylene rings that are connected by a C_2 axis are not parallel, but include angles of 69.4(2) and 78.6(1)°, respectively.

Inspection of the space-filling representation (Fig. 4, bottom) offers an impression of the steric conditions: the entrance into the boat is of sufficient size for the passage of smaller molecules like $C_2H_4Cl_2$, which is embedded tightly inside the cavity. An additional $C_2H_4Cl_2$ and a water molecule are located outside the cavity. It should be mentioned that from a solvent mixture consisting of $C_2H_4Cl_2$, (n-butyl)$_2$O, and H_2O, the chlorinated hydrocarbon is selected to be incorporated as a guest into the cavity of **6**.

Similar to **3** the macrocycles **6** are stacked in such a manner that they form channels with their cavities along the *b* axis (Fig. 5). However, in contrast to **3** the P-phenyl rings are located outside the channels, which have the shape of a flattened rhombus. Thus the passage through the channels is impeded. All four NH

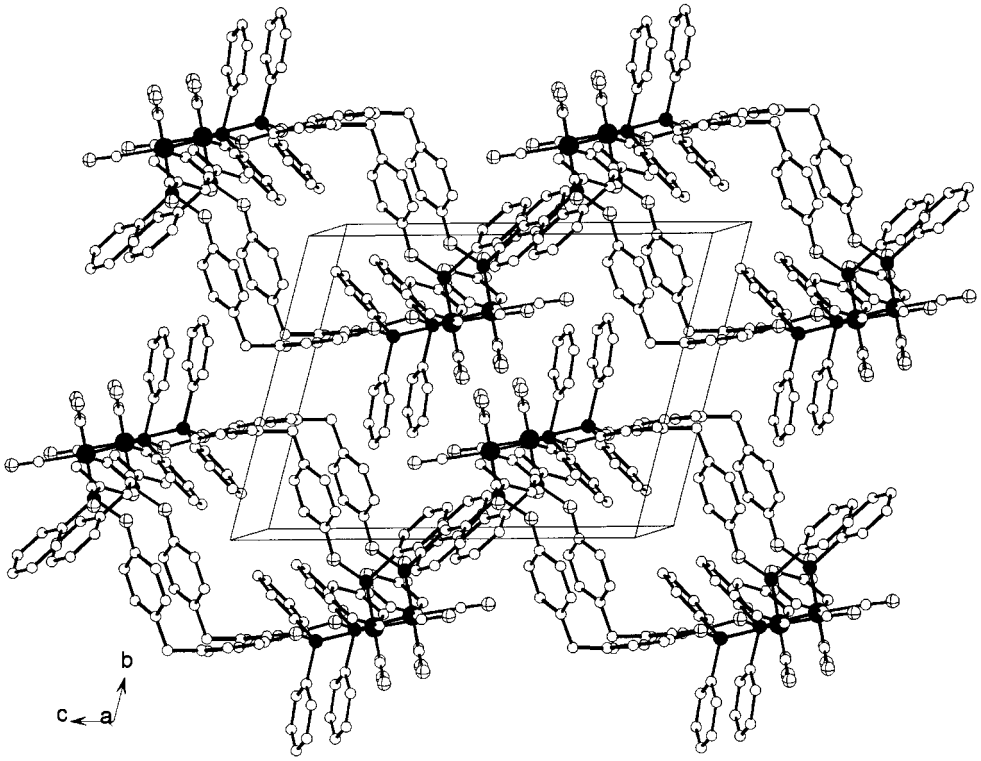

Fig. 2. Four channels of molecules in the crystal structure of **3** viewed along the *a* axis. Solvent molecules are omitted for clarity, unit cell is shown.

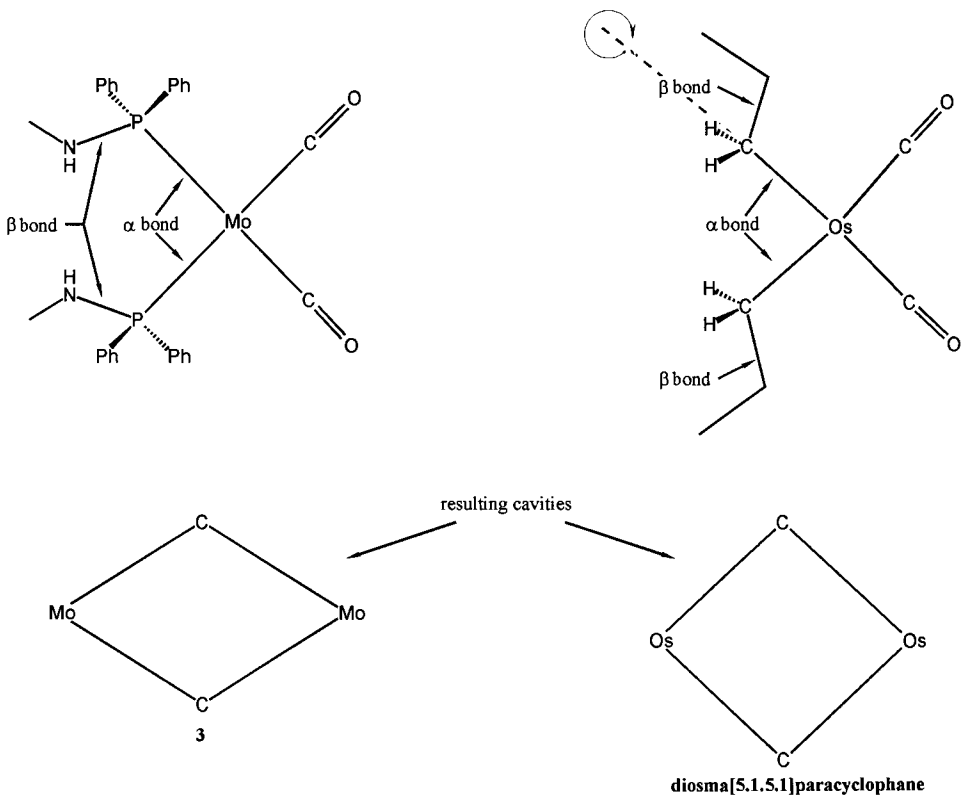

Fig. 3. Schematic view onto the transition metal fragments of compound **3** and the diosma[5.1.5.1]paracyclophane along the axial CO ligands.

functions are oriented outwards from the cavity and like in **3** a change in the conformation is a necessary precondition for the inclusion of guests via hydrogen bonding.

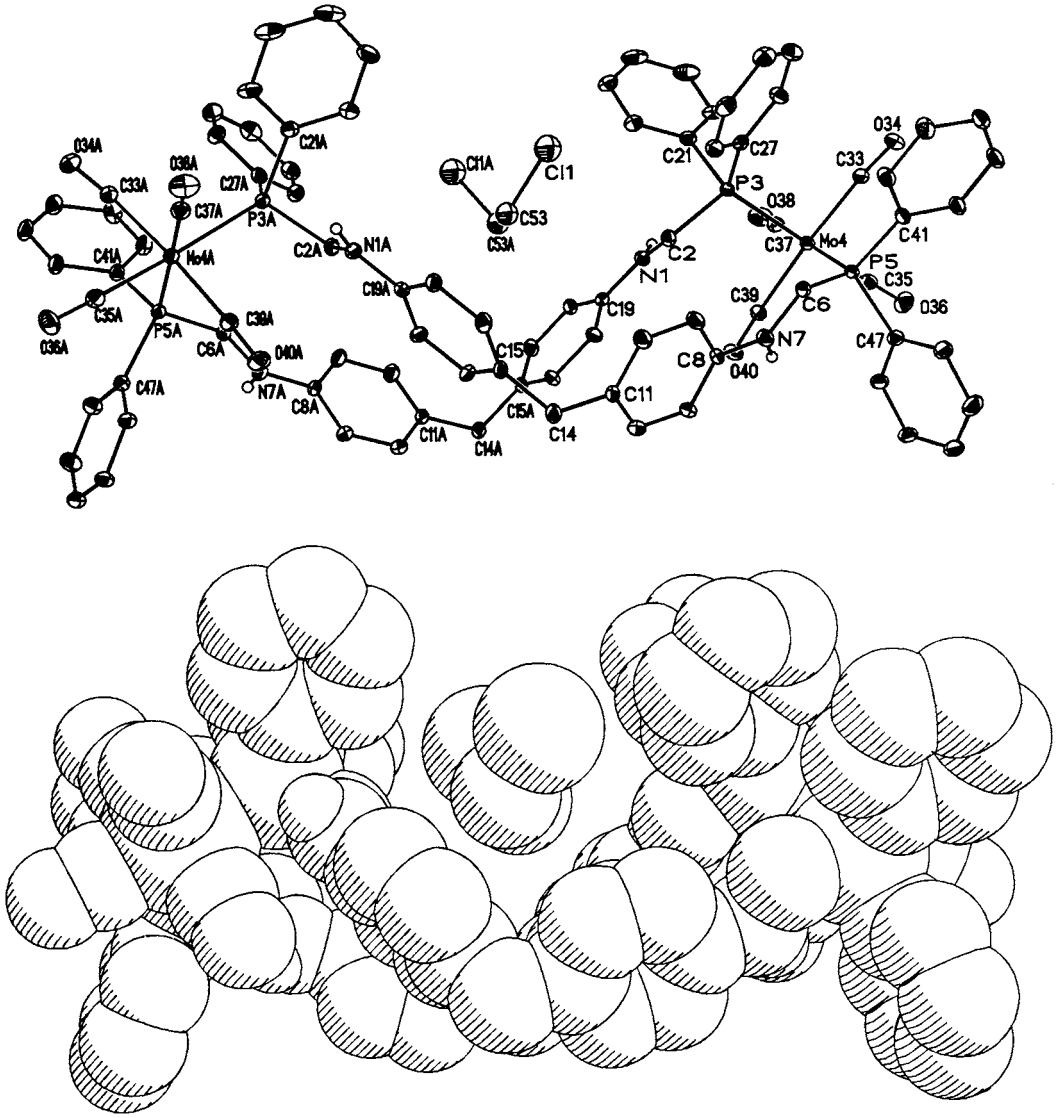

Fig. 4. Top: ORTEP plot of the molecular structure of compound **6**. Thermal ellipsoids are drawn at 20% probability level, except for H atoms. Phenyl rings are numbered cyclically. Bottom: space-filling representation of **6**. Solvent molecules that are located outside the cavity are omitted for clarity.

3. Conclusions

With regard to the possibility of forming host–guest complexes, two novel tetraphosphadimolybdacyclophanes with different ring sizes and four NH binding sites were introduced in this investigation. Satisfactory yields of the macrocycles **3** and **6** are only achieved if the aminodiphosphines **2** and **5** are reacted with (η^4-nbd)$Mo(CO)_4$ under high-dilution conditions, which is enabled by employing a computer-controlled dosing apparatus. In consideration of the fact that solvent molecules are included in the cavities of molecules **3** and **6**, inclusion experiments with hydrogen acceptors were performed in solution applying NMR titration methods [15]. The guests tested were *p*-benzoquinone, 1,4-cyclohexanedione, 2,5-piperazinedione and *trans*-1,4-diaminocyclohexane. However, none of these potential guests gave rise to separate ^{1}H-NMR peaks or to a change in the chemical shift of the respective proton signals attributed to the formation of a host–guest complex. In contrast, a similar macrocyclic system without transition metals, which was described by Hunter and co-workers, clearly features molecular recognition [16a]. The main difference between both systems is the low tendency of the molybdacyclophanes **3** and **6** to form hydrogen bonds. Because of the presence of peptide functions, the macrocycles described by Hunter and co-workers are able to provide hydrogen bonds even in water [2f].

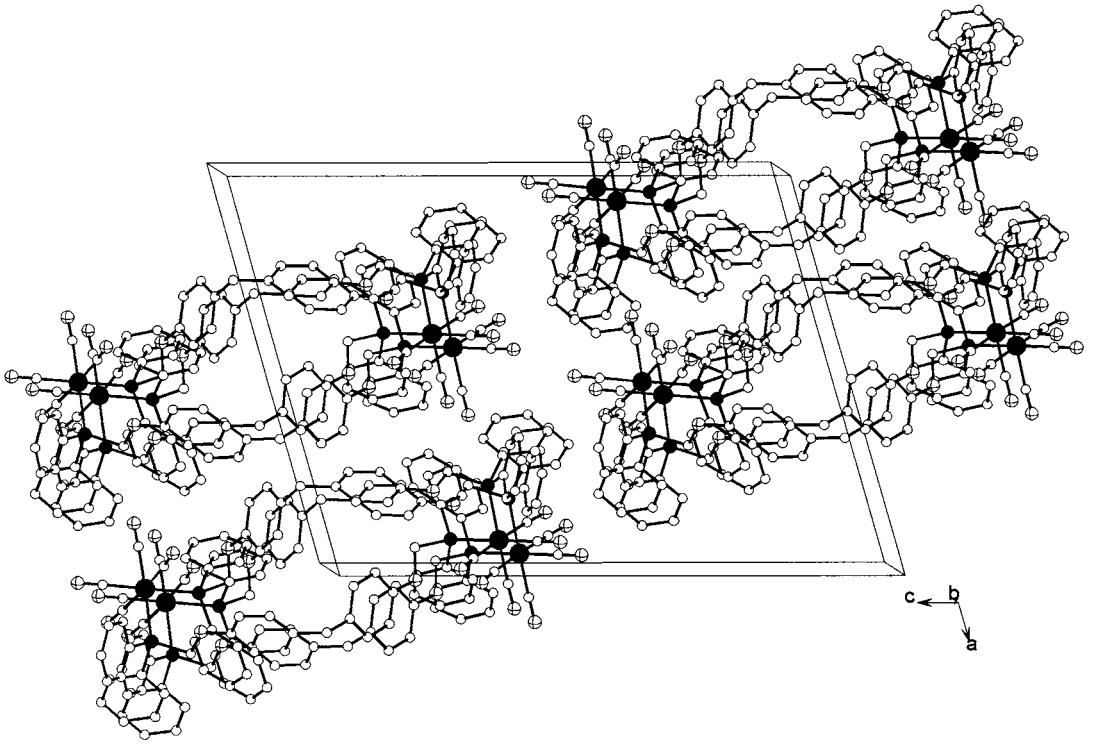

Fig. 5. Four channels of molecules of **6** viewed along the *b* axis. Solvent molecules are omitted for clarity, unit cell is shown.

4. Experimental

4.1. General procedures

All manipulations were carried out under an atmosphere of argon by use of standard Schlenk techniques. Solvents were dried with appropriate reagents, distilled, degassed, and stored under argon. IR data were obtained with Bruker IFS 48 FTIR and Bruker IFS 25 FTIR spectrometers. FD mass spectra were taken on a Finnigan MAT 711 A instrument, modified by AMD; FAB mass spectra were recorded on a Finnigan MAT TSQ 70. Elemental analyses were performed with a Elementar Vario EL analyzer; Mo was analyzed according to the literature [26]; AAS was performed on a Varian Spectra AA20 Plus spectrometer. ^{1}H-, ^{31}P{^{1}H}-, ^{31}P- and ^{13}C{^{1}H}-NMR spectra were recorded on a Bruker DRX 250 spectrometer at 250.13, 101.25, and 62.90 MHz, respectively, and at 25°C. ^{1}H and ^{13}C chemical shifts were measured relative to partially deuterated solvent peaks and to deuterated solvent peaks, respectively, which are reported relative to TMS. ^{31}P chemical shifts were measured relative to 85% H_3PO_4 ($\delta = 0$). (η^4-nbd)Mo(CO)$_4$ was obtained analogous to a literature method [27] and sublimed at 75°C (1.5×10^{-3} mbar). The diamine **1** (Merck–Schuchardt) was purified by distillation and precipitated from a CH_2Cl_2 solution with *n*-pentane. Paraformaldehyde (Merck) was dried in vacuo over P_4O_{10}. Chlorodiphenylphosphine (Fluka) was distilled and stored under argon at 4°C.

4.2. Dosing apparatus

The dosing apparatus consists of two 50 ml Hamilton gastight syringe barrels mounted on a carrier. The plungers are precisely and simultaneously moved by a step motor via a spindle. Each of the syringes is connected via a Teflon pipe to a magnetic valve with three entries that controls the direction of the flow of the solutions of the educts. Two further entries of the magnetic valves are connected to storing vessels which can be refrigerated. Another set of entries is connected to cannulas, which are penetrating compact Teflon blocks. These Teflon blocks fit into the ground joints of the reaction vessel. The step motor and the magnetic valves are computer controlled.

4.3. Chromatography

Chromatography was performed on a preparative scale with a Büchi MPLC system consisting of a B-681 chromatography pump equipped with a six-way changeover valve, a UV–vis filter–photometer and a Knauer strip chart recorder. A standard column (Ø = 49 mm, $l = 460$ mm) equipped with a precolumn and a PrepElut dry application column, for sample injection, were used. The columns were filled using a dry packing

technique (Büchi dry-filling set). Unmodified non-regular silica gel (pore size 60 Å, particle size 25–40 μm) was purchased from Machery–Nagel ('Polygoprep 60–30'), degassed and used as stationary phase. Samples were eluted isocratically by a mobile phase consisting of a 2:5 ethyl acetate–*n*-hexane mixture and the solvents were purified as described in Section 4.1. The mobile phase flow rate was fixed at 29 ml min^{-1}.

4.4. *N,N′-Bis(diphenylphosphino)4,4′-diaminodiphenylmethane (**2**)*

A solution of chlorodiphenylphosphine (3.40 g, 15.40 mmol) in 50 ml of THF was added dropwise at −10°C to a solution of **1** (1.53 g, 7.70 mmol), triethylamine (2.14 ml, 15.44 mmol) and 4-(dimethylamino)-pyridine (DMAP) (40 mg, 0.32 mmol) in 50 ml of THF. After the addition was completed precipitated $HNEt_3Cl$ was filtered (P3) and washed twice with 20 ml of THF. The solvent was evaporated in vacuo and replaced by 20 ml of CH_2Cl_2. This mixture was washed three times with 5 ml of an aqueous $NaHCO_3$ solution (5%) and then dried twice with Na_2SO_4. The product precipitated with addition of 40 ml of *n*-pentane. The remainder of the filtrate (P3) was washed twice with 10 ml of *n*-pentane and dried overnight under reduced pressure to give 4.41 g (98%) of **2**·H_2O as a colorless powder; m.p. 74.2°C (dec.). MS (FD, 30°C): *m*/*z* 566 [M^+]. Anal. Calc. for $C_{37}H_{32}N_2P_2·H_2O$ (584.63): C, 76.01; H, 5.86; N, 4.79. Found: C, 76.04; H, 6.01; N, 4.63%. IR (THF): ν(NH) = 3289 (m) cm^{-1}. $^{31}P\{^1H\}$-NMR (101.26 MHz, $CDCl_3$, 22°C): $\delta = 29.5$ (s). ^1H-NMR (250.13 MHz, $CDCl_3$, 22°C): $\delta = 3.7$ (s, 2H, C_6H_4–CH_2–C_6H_4), 4.2 (d, ^2J(PH) = 8.2 Hz, 2H, NH), 6.9, 7.0 (AB pattern, ^3J(HH) = 8.5 Hz, 8H, C_6H_4), 7.3–7.4 (m, 20H, PPh_2). $^{13}C\{^1H\}$-NMR (62.90 MHz, $CDCl_3$, 22°C): $\delta = 40.7$ (s, C_6H_4–*C*–C_6H_4), 116.5 (d, ^3J(PC) = 12.8 Hz, 3,3′,5,5′-C of C_6H_4), 128.9 (d, ^3J(PC) = 8.1 Hz, *m*-C of PPh_2), 129.5 (s, *p*-C of PPh_2), 130.0 (d, ^4J(PC) = 1.4 Hz, 2,2′,6,6′-C of C_6H_4), 131.7 (d, ^2J(PC) = 20.2 Hz, *o*-C of PPh_2), 133.2 (d, ^5J(PC) = 1.4 Hz 1,1′-C of C_6H_4), 140.8 (d, ^2J(PC) = 12.1 Hz, 4,4′-C of C_6H_4), 145.0 (d, ^1J(PC) = 17.5 Hz, *ipso*-C of PPh_2).

4.5. *N,N′-Bis[(diphenylphosphino)methyl]4,4′-diaminodiphenylmethane (**5**)*

Sodium (2.30 g, 100.00 mmol) was dissolved in 30 ml of methanol. A solution of **1** (1.98 g, 10.00 mmol) in 10 ml of methanol was added via a Teflon pipe. This mixture was stirred for 15 min giving a colorless suspension. The suspension was added to another suspension of anhydrous paraformaldehyde (0.84 g, 28.00 mmol) in 20 ml of methanol via a Teflon pipe and was stirred for a further 5 h at ambient temperature. Then the reaction mixture was pumped onto 250 ml of degassed ice-water. The aqueous phase was extracted (0°C) with 75 ml of CH_2Cl_2. This procedure was repeated twice with 25 ml of CH_2Cl_2. The CH_2Cl_2 phases were collected and dried with degassed Na_2SO_4. This CH_2Cl_2 solution was added dropwise at 0°C to a solution of diphenylphosphine (3.72 g, 20.00 mmol) in 20 ml of CH_2Cl_2. After the addition was completed, stirring was continued for 2 h at ambient temperature. Then 20 ml of toluene was added and CH_2Cl_2 and methanol were removed in vacuo. The toluene solution was filtered (P3) with a 2 cm column containing basic Al_2O_3, which was subsequently rinsed twice with 20 ml of toluene. The filtrate was transferred via a Teflon pipe to 200 ml of vigorously stirred *n*-hexane at −50°C and allowed to precipitate for 2 h. The supernatant solution was removed via a Teflon pipe and the precipitate was washed with 10 ml of *n*-pentane and dried overnight in vacuo to give 4.3 g (72%) of **5** as a colorless sticky material; m.p. 36.7°C. MS (FD, 30°C): *m*/*z* 595.6 [M^+]. Anal. Calc. for $C_{39}H_{36}N_2P_2$ (594.73): C, 78.77; H, 6.10; N, 4.71. Found: C, 78.72%; H, 6.35; N, 4.80%. IR (THF): ν(NH) = 3351 (m) cm^{-1}. $^{31}P\{^1H\}$-NMR (101.26 MHz, $CDCl_3$, 22°C): $\delta = -17.9$ (s). ^1H-NMR (250.13 MHz, $CDCl_3$, 22°C): $\delta = 3.5$ (s, 2H, NH), 3.7 (s, 2H, C_6H_4–CH_2–C_6H_4), 3.8 (d, ^3J(PH) = 3.8 Hz, N–CH_2–P), 6.5, 7.0 (AB pattern, ^3J(HH) = 8.3 Hz, 8H, C_6H_4), 7.3–7.5 (m, 20H, PPh_2). $^{13}C\{^1H\}$-NMR (62.90 MHz, $CDCl_3$, 22°C): $\delta = 41.4$ (s, C_6H_4–*C*–C_6H_4), 45.0 (d, ^2J(PH) = 11.4 Hz, N–CH_2–P), 114.5 (s, 3,3′,5,5′-C of C_6H_4), 130.0 (d, ^3J(PC) = 6.4 Hz, *m*-C of PPh_2), 130.2 (s, *p*-C of PPh_2), 130.8 (s, 2,2′,6,6′-C of C_6H_4), 132.7 (s, 1,1′-C of C_6H_4), 134.2 (d, ^2J(PC) = 18.5 Hz, *o*-C of PPh_2), 137.6 (d, ^1J(PC) = 12.8 Hz, *ipso*-C of PPh_2), 147.6 (d, ^3J(PC) = 6.4 Hz, 4,4′-C of C_6H_4).

4.6. *General procedure for the formation of the dimolybdacyclophanes **3** and **6***

A reaction vessel was charged with 500 ml of CH_2Cl_2. With the aid of a dosing apparatus, solutions of the ligands **2** or **5** and (η^4-nbd)$Mo(CO)_4$ in 200 ml of CH_2Cl_2 were slowly added within 72 h under vigorous stirring and exclusion of light at ambient temperature. After the addition was completed the solvent and norbornadiene were removed in vacuo. The remainder was suspended in 20 ml of CH_2Cl_2 (**3**) or $CHCl_3$ (**6**) and the suspension was filtered (P3) over a 5 cm layer of silica, which was subsequently rinsed with 300 ml of CH_2Cl_2 (**3**) or $CHCl_3$ (**6**). To the filtrates 8.0 g of silica gel was added and the solvent was removed in vacuo. The remaining silica was filled into a PrepElut dry application column and compressed at 10 bar (N_2) according to a Büchi procedure using a dry-filling set [28]. After MPLC the eluent was removed in vacuo. The remain-

der was dissolved in 100 ml of CH_2Cl_2 (**3**) or $CHCl_3$ (**6**), precipitated with 200 ml of *n*-pentane and finally the products were washed with 10 ml of *n*-pentane.

*4.7. 3,3,3,3,21,21,21,21-Octacarbonyl-2,2,4,4,20,20,22,22-octaphenyl-1,5,19,23-tetraaza-2,4,20,22-tetraphospha-3,21-dimolybda[5.1.5.1]paracyclophane (**3**)*

Starting materials: **2** (1.98 g, 3.50 mmol) and (η^4-nbd)$Mo(CO)_4$ (1.05 g, 3.50 mmol). Purification by MPLC afforded **3** as the fraction with the highest peak intensity ($t_R = 17$ min). Yield: 1.41 g (26%) of **3**; colorless powder; m.p. 199.9°C. MS (FAB, 30°C, negative ions): *m*/*z* 1548.7 [M^+]. Anal. Calc. for $C_{82}H_{64}Mo_2N_4O_8P_2 \cdot H_2O$ (1567.22): C, 62.84%; H, 4.24%; Mo, 12.24%; N, 3.57%. Found: C, 62.54%; H, 4.24%; Mo, 11.76%; N, 3.56%. IR (THF): ν(NH) = 3389 (w), 3245 (w) cm^{-1}. IR (CCl_4): ν(CO) = 2023 (m), 1930 (s), 1899 (s), 1880 (vs) cm^{-1}. $^{31}P\{^1H\}$-NMR (101.26 MHz, $CDCl_3$, 22°C): $\delta = 72.5$ (s). ^{1}H-NMR (250.13 MHz, $CDCl_3$, 22°C): $\delta = 3.4$ (s, 4H, C_6H_4–CH_2–C_6H_4), 4.7 (m, N = 20.7 Hz[2] [29], 4H, NH), 6.0, 6.6 (AB pattern, ^3J(HH) = 8.3 Hz, 16H, C_6H_4), 7.4–7.7 (m, 40H, PPh_2). $^1H\{^{31}P\}$-NMR (250.13 MHz, 101.26 $CDCl_3$, 22°C): $\delta = 4.7$ (s, 4H, NH). $^{13}C\{^1H\}$-NMR (62.90 MHz, $CDCl_3$, 22°C): $\delta = 41.2$ (s, C_6H_4–*C*–C_6H_4), 120.9 (s, 3,3′,5,5′-C of C_6H_4), 131.1 (m, N = 10.0 Hz[3] [29], *m*-C of PPh_2), 131.3 (s, *p*-C of PPh_2), 132.4 (s, 1,1′-C of C_6H_4), 133.6 (m, N = 12.8 Hz[3] [29], *o*-C of PPh_2), 136.8 (s, 2,2′,6,6′-C of C_6H_4), 138.7 (m, N = 38.4 Hz[3] [29], *ipso*-C of PPh_2), 142.6 (m, N = 11.4 Hz[3] [29], 4,4′-C of C_6H_4), 209.5 (t, ^2J(PC) = 9.8 Hz, CO_{ax}), 214.6 (m, N = 19.5 Hz [29][3], CO_{eq}).

*4.8. 4,4,4,4,24,24,24,24-Octacarbonyl-3,3,5,5,23,23,25,25-octaphenyl-1,7,21,27-tetraaza-3,5,23,25-tetraphospha-4,24-dimolybda[7.1.7.1]paracyclophane (**6**)*

Starting materials: **5** (2.08 g, 3.50 mmol) and (η^4-nbd)$Mo(CO)_4$ (1.05 g, 3.50 mmol). Purification by MPLC afforded **6** as the fraction with the highest peak intensity ($t_R = 29$ min). Yield: 1.32 g (23.5%) of **6**; colorless powder; m.p. 164.3°C. MS (FD, 30°C): *m*/*z* = 1606.1 [M^+]. Anal. Calc. for $C_{86}H_{72}Mo_2N_4O_8 \cdot 1.5CH_2Cl_2$ (1732.7): C, 60.65; H, 4.36; Cl, 6.14; Mo, 11.07; N, 3.23. Found: C, 60.96; H, 4.50; Cl, 5.88; Mo, 10.80; N, 3.23%. IR (THF): ν(NH) = 3380 (m) cm^{-1}. IR (acetone): ν(CO) = 2021 (m), 1920 (s), 1907 (vs), 1884 (s) cm^{-1}. $^{31}P\{^1H\}$-NMR (101.26 MHz, $CDCl_3$, 22°C): $\delta = 29.2$ (s). ^{1}H-NMR (250.13 MHz, $CDCl_3$, 22°C): $\delta = 3.4$ (dt, ^3J(HH) = 5.5 Hz, ^4J(PH) = 4.9 Hz, 4H, NH), 3.6 (s, 4H, C_6H_4–CH_2–C_6H_4), 3.7 (d, ^2J(PH) = 5.6 Hz, 8H, N–CH_2–P), 6.1, 6.8 (AB pattern, ^3J(HH) = 8.3 Hz, 16H, C_6H_4), 7.3–7.4 (m, 40H, PPh_2). $^1H\{^{31}P\}$-NMR (250.13 MHz, 101.26 $CDCl_3$, 22°C): $\delta = 3.5$ (t, ^3J(HH) = 5.5 Hz, 4H, NH). $^{13}C\{^1H\}$-NMR (62.90 MHz, $CDCl_3$, 22°C): $\delta = 41.7$ (s, C_6H_4–*C*–C_6H_4), 32.3 (s, N–CH_2–P), 115.0 (s, 3,3′,5,5′-C of C_6H_4), 130.4 (m, N = 9.1 Hz[3] [29], *m*-C of PPh_2), 130.9 (s, *p*-C of PPh_2), 131.6 (s, 1,1′-C of C_6H_4), 133.7 (s, 2,2′,6,6′-C of C_6H_4), 133.8 (m, N = 11.5 Hz[3] [29], *o*-C of PPh_2), 136.4 (m, N = 32.7 Hz[3] [29], *ipso*-C of PPh_2), 147.2 (m, N = 7.7 Hz[3] [29], 4,4′-C of C_6H_4), 211.4 (t, ^2J(PC) = 9.1 Hz, CO_{ax}), 216.0 (m, N = 16.2 Hz[3] [29], CO_{eq}).

4.9. Crystallographic analysis

Colorless single crystals suitable for X-ray structural determinations were obtained by slow evaporation of a solution of **3** in $CHCl_3$ and diffusion of di-*n*-butyl ether into a solution of **6** in dichloroethane, respectively. The crystals were mounted on a glass fiber and transferred to a P4 Siemens diffractometer, using graphite-monochromated Mo–K_α radiation. Random searches were performed to find suitable reduced cells. The lattice constants were determined by 25 (**3**) and 29 (**6**) precisely centered high-angle reflections and refined by least-square methods. The final cell parameters for **3** and **6** are summarized in Table 3. Intensities were collected via the ω-scan technique. Absorption corrections were applied (Ψ-scan). The resultant data of **3** fit best with the triclinic space group $P\bar{1}$ with one formula unit per unit cell ($Z = 1$) and six distorted chloroform molecules. **6** crystallizes in the monoclinic space group $C2$ ($Z = 2$) with two molecules of 1,2-dichloroethane and one molecule of water. The structures were solved by direct methods with SHELXS [30] and refined by least squares using SHELXTL with anisotropic thermal parameters for all non-hydrogen atoms except the solvent molecules (based on F^2) [31]. Hydrogen atoms were included in calculated positions (riding model) with exception of water and the distorted $CHCl_3$ molecules. The maximum and minimum peaks in the final difference synthesis were 1.894, −2.224 (**3**), and 1.133, −1.586 (**6**) e $Å^{-3}$, respectively.

5. Supplementary material

Crystallographic data for the structures reported in this paper have been deposited with the Cambridge Crystallographic Data Centre as supplementary publication nos. CCDC 130862 for **3** and CCDC 130863 for **6**. Copies of the data can be obtained free of charge on application to CCDC, 12 Union Road, Cambridge, CB2 1EZ, UK (Fax: +44-1223-336033; e-mail: deposit@ccdc.cam.ac.uk).

[2] AA′XX′ spin system, $N = |^2J(PH) + {}^4J(PH)|$.

[3] A part of an AXX′ spin system, $N = |^mJ(AX) + {}^nJ(AX')|$.

Table 3
Crystallographic data and refinement details for **3** and **6**

	Compound **3**·6$CHCl_3$	Compound **6**·2$C_2H_4Cl_2$·H_2O
Empirical formula	$C_{88}H_{70}Cl_{18}Mo_2N_4O_8P_4$	$C_{90}H_{82}Cl_4Mo_2N_4O_9P_4$
Formula weight	2265.34	1821.16
Temperature (K)	173(2)	173(2)
Wavelength, Mo–K_α (Å)	0.71073	0.71073
Crystal system	Triclinic	Monoclinic
Space group	$P\bar{1}$	$C2$
a (Å)	11.235(2)	17.935(3)
b (Å)	13.154(2)	10.097(3)
c (Å)	17.218(2)	24.220(4)
α (°)	105.33(1)	90
β (°)	94.27(1)	105.78(1)
γ (°)	90.80(1)	90
V (Å^3)	2445.7(6)	4221(2)
Z	1	2
$D_{calc.}$ (g cm^{-3})	1.538	1.433
Absorption coefficient (mm^{-1})	0.868	0.560
$F(000)$	1140	1868
Crystal size (mm)	$0.30\times0.20\times0.20$	$0.30\times0.20\times0.10$
θ Range for data collection (°)	2–27.5	2–27.5
Index ranges	$-14\le h\le14,\ -16\le k\le16,\ -22\le l\le22$	$-23\le h\le23,\ -13\le k\le1,\ -31\le l\le30$
Reflections collected	14553	11275
Independent reflections	889 ($R_{int}=0.0227$)	5686 ($R_{int}=0.1070$)
Refinement method	Full-matrix least-squares on F^2	Full-matrix least-squares on F^2
Data/restraints/parameters	8891/0/541	5686/3/487
Goodness of fit on F^2	1.671	1.878
Final R indices [$I>2\sigma(I)$]	$R_1=0.0867$ [a], $wR_2=0.2229$ [b]	$R_1=0.0529$ [a], $wR_2=0.1301$ [b]
R indices (all data)	$R_1=0.0980$ [a], $wR_2=0.2417$ [b]	$R_1=0.0601$ [a], $wR_2=0.1400$ [b]
Largest diff. peak and hole e Å^{-3}	1.894 and −2.224	1.133 and −1.586
Max. and min. transmission	0.8455 and 0.7807	0.3707 and 0.3253

[a] $R_1=\Sigma\|\|F_o\|-\|F_c\|\|/\Sigma|F_o|$.
[b] $wR_2=[\Sigma[w(F_o^2-F_c^2)^2]/\Sigma[w(F_o^2)^2]]^{0.5}$.

Acknowledgements

Support of this research by the Deutsche Forschungsgemeinschaft and the Fonds der Chemischen Industrie is gratefully acknowledged. We are also indebted to Priv.-Doz. Dr H.A. Mayer, Institut für Anorganische Chemie II, University of Tübingen, for helpful discussions regarding the interpretation of the NMR spectra.

References

[1] E. Lindner, C. Hermann, G. Baum, D. Fenske, Eur. J. Inorg. Chem. (1999) 679.
[2] (a) J.L. Atwood, J.E.D. Davies, D.D. MacNicol, F. Vögtle (Eds.), Comprehensive Supramolecular Chemistry, vol. 2, Pergamon, Oxford, 1996. (b) J.-M. Lehn, Supramolecular Chemistry, VCH, Weinheim, 1995. (c) F. Diederich, Cyclophanes, The Royal Society of Chemistry, Cambridge, 1991. (d) F. Vögtle, Cyclophan-Chemie, Teubner, Stuttgart, 1990. (e) M. Inouye, K. Fujimoto, M. Furusyo, H. Nakazumi, J. Am. Chem. Soc. 121 (1999) 1452. (f) C. Allot, H. Adams, P.L. Bernad, Jr., C.A. Hunter, C. Rotger, J.A. Thomas, Chem. Commun. (Cambridge) (1998) 2449. (g) S.M. Ngola, P.C. Kearney, S. Mecozzi, K. Russell, D.A. Dougherty, J. Am. Chem. Soc. 121 (1999) 1192.
[3] (a) C.D. Gutsche, Calixarenes Revisited, The Royal Society of Chemistry, Cambridge, 1998. (b) C.D. Gutsche, Calixarenes, The Royal Society of Chemistry, Cambridge, 1989. (b) A. Ikeda, S. Shinkai, Chem. Rev. 97 (1997) 1713.
[4] (a) A. Collet, J.-P. Dutasta, B. Lozach, J. Canceill in: M.J.S. Dewar, J.D. Dunitz, K. Hafner, S. Ito, J.-M. Lehn, K.N. Raymond, C.W. Rees, J. Thiem, F. Vögtle (Eds.), Cyclotriveratrylenes and Cryptophanes: Their Synthesis and Applications to Host–Guest Chemistry and to the Design of New Materials: Topics in Current Chemistry, vol. 165, Springer, Heidelberg, 1993. (b) M. Luhmer, B.M. Goodson, Y.-Q. Song, D.L. Laws, L. Kaiser, M.C. Cyrier, A. Pines, J. Am. Chem. Soc. 121 (1999) 3502.
[5] (a) D.J. Cram, J.M. Cram, Container Molecules and Their Guests, The Royal Society of Chemistry, Cambridge, 1994. (b) A. Jasat, J.C. Sherman, Chem. Rev. 99 (1999) 931.
[6] (a) B. Olenyuk, A. Fechtenkötter, P.J. Stang, J. Chem. Soc. Dalton Trans. (1998) 1707. (b) M. Fujita, D. Oguro, M. Miyazawa, H. Oka, K. Yamaguchi, K. Ogura, Nature 378 (1995) 469. (c) P.N.W. Baxter, J.-M. Lehn, G. Baum, D. Fenske, Chem. Eur. J. 5 (1999) 103. (d) P.N.W. Baxter, J.-M. Lehn, B.O. Kneisel, G. Baum, D. Fenske, Chem. Eur. J. 5 (1999) 113.
[7] (a) I.A. Bagatin, D. Matt, H. Thönnessen, P.G. Jones, Inorg. Chem. 38 (1999) 1585. (b) P. Molenveld, J.F.J. Engbersen, H. Kooijman, A.L. Spek, D.N. Reinhoudt, J. Am. Chem. Soc. 120 (1998) 6726. (c) H.K.A.C. Coolen, J.A.M. Meeuwis, P.W.N.M. van Leeuwen, R.J.M. Nolte, J. Am. Chem. Soc. 117 (1995) 11906.

[8] (a) E. Lindner, I. Krebs, R. Fawzi, M. Steimann, Organometallics 18 (1999) 480. (b) F.S. McQuillan, C.J. Jones, Polyhedron 15 (1996) 1533.
[9] (a) J. Vaugeois, M. Simard, J.D. Wuest, Organometallics 17 (1998) 1215. (b) M.T. Reetz, C.M. Niemeyer, M. Hermes, R. Goddard, Angew. Chem. 104 (1992) 1054; Angew. Chem. Int. Ed. Engl. 31 (1992) 1017.
[10] R.V. Slone, D.I. Yoon, R.M. Calhoun, J.T. Hupp, J. Am. Chem. Soc. 117 (1995) 11813.
[11] M.B. Inoue, E.F. Velazquez, F. Medrano, K.L. Ochoa, J.C. Galvez, M. Inoue, Q. Fernando, Inorg. Chem. 37 (1998) 4070.
[12] C.J. Jones, Chem. Soc. Rev. 27 (1998) 289.
[13] (a) J.R. Farrell, C.A. Mirkin, I.A. Guzei, L.M. Liable-Sands, A.L. Rheingold, Angew. Chem. 110 (1998) 484; Angew. Chem. Int. Ed. Engl. 37 (1998) 465. (b) K. Fujimoto, S. Shinkai, Tetrahedron Lett. 35 (1994) 2915.
[14] (a) E. Lindner, M.W. Pitsch, R. Fawzi, M. Steimann, Chem. Ber. 129 (1996) 639. (b) E. Lindner, W. Wassing, R. Fawzi, M. Steimann, Angew. Chem. 106 (1994) 363; Angew. Chem. Int. Ed. Engl. 33 (1994) 321. (c) E. Lindner, W. Wassing, M.W. Pitsch, R. Fawzi, M. Steimann, Inorg. Chim. Acta 220 (1994) 107.
[15] E. Lindner, M.F. Günther, H.A. Mayer, R. Fawzi, M. Steimann, Chem. Ber. Recueil 130 (1997) 1815.
[16] (a) H. Adams, F.J. Carver, C.A. Hunter, N.J. Osborne, Chem. Commun. (Cambridge) (1996) 2529. (b) F.S. McQuillan, H. Chen, T.A. Hamor, C.J. Jones, H.A. Jones, R.P. Sidebotham, Inorg. Chem. 38 (1999) 1555. (c) M. Fujita, S. Nagao, M. Iida, K. Ogata, K. Ogura, J. Am. Chem. Soc. 115 (1993) 1574.
[17] T.Q. Ly, A.M.Z. Slawin, J.D. Woollins, J. Chem. Soc. Dalton Trans. (1997) 1611.
[18] A. Tarassoli, R.C. Haltiwanger, A.D. Norman, Inorg. Chem. 21 (1982) 2684.
[19] (a) J. Barluenga, A.M. Bayón, P. Campos, G. Asensio, E. Gonzalez-Nuñez, Y. Molina, J. Chem. Soc. Perkin Trans. I (1988) 1631. (b) J. Barluenga, P.J. Campos, G. Canal, G. Asensio, Synlett (1990) 261.
[20] (a) L. Rossa, F. Vögtle in: F. Vögtle (Ed.), Synthesis of Medio- and Macrocyclic Compounds by High Dilution Principle Techniques: Topics in Current Chemistry, vol. 113, Cyclophanes I, Springer, Heidelberg, 1983. (b) P. Knops, N. Sendhoff, H.-B. Mekelburger, F. Vögtle in: E. Weber, F. Vögtle (Eds.), High Dilution Reactions — New Synthetic Applications: Topics in Current Chemistry, vol. 161, Macrocycles, Springer, Heidelberg, 1992.
[21] S. Karbach, W. Löhr, F. Vögtle, J. Chem. Res. (S) (1981) 314; J. Chem. Res. (M) (1981) 3579.
[22] C. Kayran, F. Kozanoglu, S. Özkar, S. Saldamli, A. Tekkaya, C.G. Kreiter, Inorg. Chim. Acta 284 (1999) 229.
[23] S. Berger, S. Braun, H.-O. Kalinowski, NMR-Spektroskopie von Nichtmetallen, Georg Thieme Verlag, Stuttgart, 1993.
[24] D. Pohl, J. Ellermann, F.A. Knoch, M. Moll, W. Bauer, J. Organomet. Chem. 481 (1994) 259.
[25] S.A. Jackson, O. Eisenstein, J.D. Martin, A.C. Albeniz, R.H. Crabtree, Organometallics 10 (1991) 3062.
[26] (a) D.J. David, Analyst 86 (1961) 730. (b) T.V. Ramakrishna, P.W. West, J.W. Robinson, Anal. Chim. Acta 44 (1969) 437. (c) G.D. Kirkbright, A.M. Smith, T.S. West, Analyst 91 (1966) 700.
[27] A. Tekkaya, C. Kayran, S. Özkar, C.G. Kreiter, Inorg. Chem. 33 (1994) 2439.
[28] A. Talamona, E. Stump, Präparative Mitteldruck-Flüssigchromatographie (MPLC); Teil 1: Die Adsorptions-Chromatographie, Büchi Laboratoriums-Technik GmbH, Göppingen, Germany.
[29] R.K. Harris, Can. J. Chem. 42 (1964) 2275.
[30] G.M. Sheldrick, Acta Crystallogr. Sect. A 51 (1995) 33.
[31] G.M. Sheldrick, SHELXTL V5.03, Program for Crystal Structure Refinement, University of Göttingen, Germany, 1997.